

CFD INVESTIGATION OF WIRE-WRAPPED FUEL ROD BUNDLES AND FLOW SENSITIVITY TO BUNDLE SIZE

L.M. Brockmeyer, F.S. Sarikurt, Y.A. Hassan

Department of Nuclear Engineering
Texas A&M University
253 Bizzell Hall West, College Station, TX 77843 USA
lbrockmeyer@tamu.edu

E. Merzari

Argonne National Laboratory
9700 S Cass Ave, Argonne, IL 60439 USA

ABSTRACT

The development of a meshing and simulation procedure for the modeling of a 19 pin wire-wrapped fuel rod bundle is detailed. Parameters varied include base size, prism layer thickness, inlet condition and turbulence model. Care was taken to ensure the flow was highly resolved around walls, and the use of wall functions was avoided. The model was validated against established pressure drop correlations. The meshing and simulation procedure was then used to model 19, 37, and 61 pin fuel rod bundles. Again the pressure drops were compared against and agreed favorably with established pressure drop correlations. The velocity distributions of each bundle were found and analyzed qualitatively and quantitatively to determine at what bundle size interior subchannel velocity distribution can be considered independent of bundle size. A qualitative look at the velocity profiles indicates that the interior subchannels of each bundle were affected by the walls. The quantitative analysis reveals that for interior subchannels, the difference is negligible for certain subchannels. Results indicate that the velocity of the 19 pin bundles centermost subchannels agree within 1% with the corresponding subchannels of the 61 pin bundle, and are thus considered independent of bundle size. The two innermost layers of subchannels in the 37 pin bundle are similarly independent of bundle size. A single layer of subchannels acting as a buffer to wall effects was sufficient to isolate interior subchannels from wall effects.

KEYWORDS

Wire-wrap, SFR, Bundle Sensitivity

1. INTRODUCTION

A common fuel arrangement for Sodium Fast Reactor designs is a hexagonal array of wire wrapped fuel rods. The helically wound wires redirect coolant to neighboring subchannels and encourage mixing. The increased mixing of the coolant is beneficial to heat transfer from the fuel and prevents temperature peaking in hot channels that may occur. Additionally, the wire-wrappers separate the rods and reduce flow-induced vibrations that cause reactivity fluctuations and may result in mechanical failure of the fuel cladding. However, wire-wrappers contribute an additional source of pressure drop through the core compared to bare rods or rods with spacer grids. Pressure drop is a key characteristic of core design and must be well understood for design optimization.

Reactors utilizing wire wrapped fuel bundles typically contain bundles of up to 217 rods. When designing models or experiments, it is often convenient to study smaller bundles containing 19, 37, or 61 rods. However care must be taken to ensure that the use of smaller bundles does not significantly affect the behavior of the fluid flow.

1.1. Literature

Only recently have computational tools become advanced enough to model core coolant flow with high detail and resolution. Historically core design was performed entirely with the use of subchannel based codes. The subchannel approach involves averaging flow characteristics such as velocity, temperature, and pressure over discrete axial segments. Conservation of mass, momentum and energy are then solved over the entire reactor volume to obtain temperature velocity distributions. The inter-channel mixing terms are obtained semi-empirically [1]. While subchannel based codes can capture temperature distribution over an entire core, their ability to capture axial variation and edge channel effects caused by wire-wrappers is limited [2].

Computational Fluid Dynamics (CFD) has become increasingly relevant to core design. Wire-wrapped bundles especially can benefit from the increased fidelity and resolution that come with CFD because of the complex geometry involved. Literature reveals that investigations into wire-wrapped fuel rods have primarily involved comparison of turbulence models and investigation of simplifying assumptions. The effects of wire wrapper shape have been investigated by Hamman and Berry [3] and Raza and Kim [4]. A variety of flow configurations were studied by Natesan et al [5]. Fischer utilized an LES turbulence modeling approach [6]. The effects of mesh density and flow conditions were investigated by Smith [7]. The effects of different pin-wire contact models was investigated by Merzari [8].

Most relevant to this investigation is the CFD investigation of 7, 19, and 37 fuel pin bundles performed by Gajapathy [9]. This investigation used RANS turbulence models with wall functions to investigate the behavior of flow through a variety of bundle sizes. Due to computational restrictions a grid dependence study was not possible. The results indicated that a 19 pin bundle is the minimum domain size that captures all important flow phenomena.

Several empirical models have been created to predict pressure drop for a wide range of wire-wrapped fuel rod bundle geometries. The correlations used in this investigation are Rheme [10], Novendstern [11], and detailed Chen and Todreas [12].

1.2. Purpose

The purpose of this investigation is to perform a more rigorous investigation of the effect of wire-wrapped fuel rod bundle size on pressure drop. Great effort was put into developing a meshing procedure which is validated against established empirical correlations. A high resolution boundary layer was created in order to avoid the use of wall functions in order to better capture the wall effects. The velocity profile and turbulent viscosity ratio profile were qualitatively compared. The average subchannel velocities for each bundle were compared to determine how large a bundle must be to sufficiently insulate inner subchannels from the effects of the shroud on velocity distribution.

2. MESH AND MODEL DETERMINATION AND VALIDATION

This section outlines the method followed to create a meshed domain for a 19 pin wire-wrapped fuel rod bundle. A thorough comparison of meshes and modeling parameters with varying base size, prism layer thickness, inlet conditions, and turbulence models was conducted in order to create a meshing and

simulation procedure with valid results. This procedure should then be valid for bundles of increased size.

2.1. CAD Model

The fuel bundle modeled consists of 19 pins arranged in a hexagonal lattice surrounded by a hexagonal shroud. The fluid domain consists of the volume outside of the fuel rods and within the shroud. Two domains were created: one with height corresponding to a full helical pitch, and one with height corresponding to $1/6^{\text{th}}$ of a helical pitch. The initial solid model of the fluid domain was created using a computer aided design software. The wire wrapped fuel rods consist of a rod with a helically wrapped wire with a circular cross section. In order to avoid point contact between the wire and neighboring pins, the pitch was increased slightly. Point contact between rod and wire wrap was avoided by approximating the wall wire attachment with fillets of small diameter. The geometric parameters used to create the model are given in Table I. The geometric parameters for the fuel bundle are shown in figure 1. The solid and fluid models of the wire wrapper bundle are shown for one full pitch in figure 2.

Table I. Characteristic Dimension for 19 Pin Bundle

Parameter	Symbol	Value
Helical Pitch	P_H	261.96 mm
Wall Length	L_W	22.715 mm
Pin to Pin Pitch	P	8.4 mm
Pin Diameter	D	6.55 mm
Wire Diameter	D_w	1.75 mm
Fillet Diameter	D_f	0.25 mm

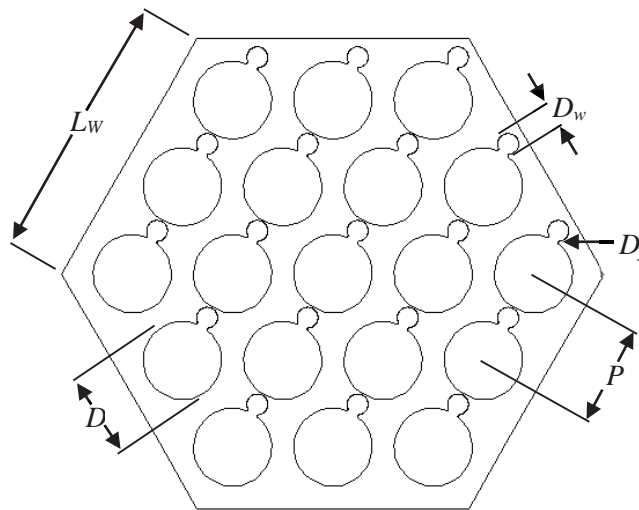


Figure 1. Geometrical meaning of characteristic parameters

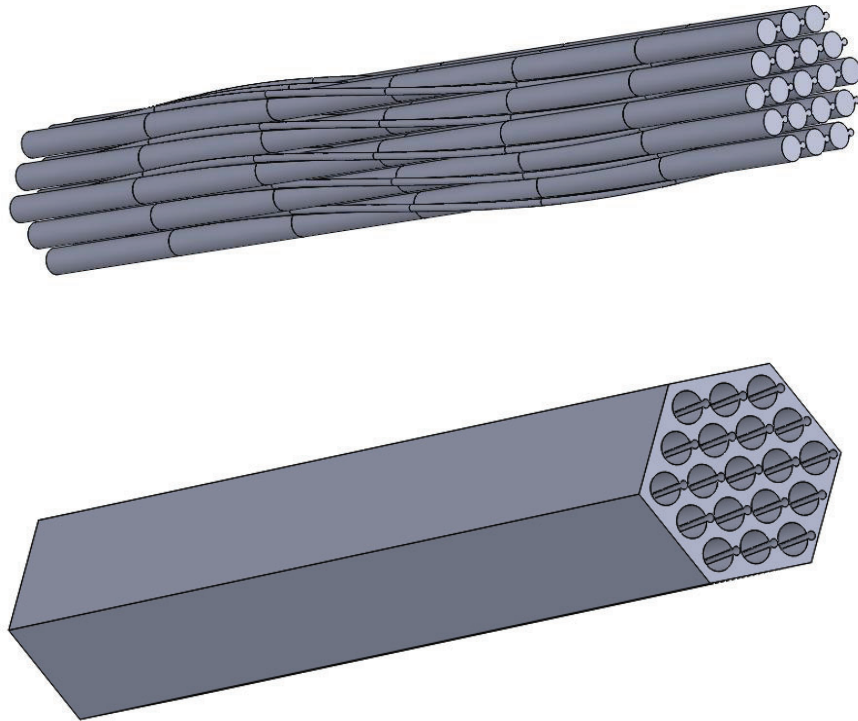


Figure 2. Solid (top) and fluid (bottom) models

2.2. Modeling Parameters

There is a lack of high-fidelity experimental data to use for validation purposes. Several empirical models of pressure drop through wire-wrapped fuel rods do exist including Rheme, Novendstern (Nov.), and Chen and Todreas (C&T). Comparison of simulated pressure drop to these three empirical models act as the primary means of validation against experiment. While all three empirical models were used for estimates, comparisons were made against the Chen and Todreas model, as literature has shown it to be the most accurate [13] [14]. An average flow rate of 2 m/s was selected in order to ensure a sufficiently high Reynolds number for turbulent flow. Three initial turbulence models were chosen as candidates for the study: standard $k-\epsilon$ Low-Re with low y^+ wall treatment (st. $k-\epsilon$), realizable $k-\epsilon$ two-layer with all y^+ wall treatment (re. $k-\epsilon$), and SST (Menter) $k-\omega$ with low y^+ treatment (SST $k-\omega$). The pressure drop through a wire-wrapped fuel rod bundle depends highly on wall interactions. Great care was taken to ensure the wall velocity profile was resolved with minimal use of wall functions. The parameter y^+ can be used to determine if the wall boundary is sufficiently resolved. Values of y^+ less than 1 are necessary for low y^+ wall treatment to resolve the viscous sublayer. The mesh was generated using a polyhedral mesher with prism layers. The domain for the models is $1/6^{\text{th}}$ of a helical pitch, as this distance is the minimum necessary to capture all of the geometry.

The fluid modeled was sodium with a fixed temperature at 700 K. The density is held constant at 852 kg/m^3 and the kinematic viscosity is held constant at $2.64\text{E-}4 \text{ Pa}\cdot\text{s}$ [15].

The inlet conditions were generated by modeling one full helical pitch with base size 0.3 mm, 5 prism layers with prism layer thickness of 0.1 mm. This model, although not validated, served to provide a non-uniform inlet condition with an average velocity of 2 m/s and no slip wall conditions. This inlet condition

was necessary to ensure that the models studied did not suffer from non-physical y^+ values at the entrance.

2.3. Spatial Convergence

The first step to determining effective modeling parameters was to establish the maximum base size that satisfied spatial convergence. All three turbulence models were utilized with base sizes 0.1, 0.15, 0.2, 0.3 mm. For these cases 10 prism layers were used with prism layer thickness of 0.1 mm. Unless otherwise noted, default values were used. Figure 3 depicts the outlet cross section mesh for each base size. The same mesh was used for each turbulence model. Table II. details the results for each turbulence model and base size, including pressure drop, percent difference from Chen and Todreas correlation, elements in mesh, approximate residuals, maximum y^+ value, and average y^+ value.

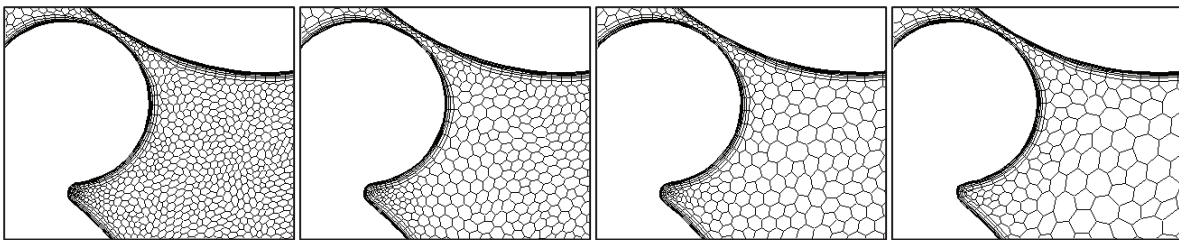


Figure 3. Mesh samples. Base size left to right: 0.1 mm, 0.15 mm, 0.2 mm, 0.3 mm

Table II. Spatial Convergence Results

Turbulence Model	Base Size (mm)	Pressure Drop (Pa/cm)	% difference from C&T	Elements (million)	Residuals	Max y^+	Avg. y^+
St. $k-\epsilon$	0.1	71.9	20.3	70.5	<1	0.64	0.19
	0.15	70.5	21.8	29.3	<1	0.79	0.19
	0.2	68.0	24.6	16.3	<1	0.61	0.18
	0.3	65.7	27.2	9.3	<1	0.48	0.18
SST $k-\omega$	0.1	88.0	2.6	70.5	<1E-4	0.90	0.33
	0.15	85.2	5.6	29.3	<1E-4	1.10	0.32
	0.2	81.1	10.2	16.3	<1E-5	1.16	0.32
	0.3	76.7	15.0	9.3	<1E-5	0.96	0.30
Re. $k-\epsilon$	0.1	101.0	11.9	70.5	<1E-3	0.89	0.35
	0.15	99.4	10.1	29.3	<1E-3	1.09	0.35
	0.2	97.6	8.1	16.3	<1E-3	1.17	0.36
	0.3	95.1	5.3	9.3	<1E-3	0.96	0.35
C&T	-	90.3	-	-	-	-	-
Nov.	-	103.5	14.6	-	-	-	-
Rehme	-	93.3	3.4	-	-	-	-

The base size convergence study reveals that st. $k-\epsilon$ is a poor candidate for this study. It far under-predicts pressure drop according to all of the pressure drop correlations by more than 20%. Additionally, its residuals are very poor. The remaining study disregards the st. $k-\epsilon$ turbulence model. Both the SST $k-\omega$

and the Re. $k-\epsilon$ results are satisfactory, with differences less than 15% for all cases. The SST $k-\omega$ results have lower residuals than the Re. $k-\epsilon$, however both are acceptable.

The primary purpose of this comparison was to determine what base size would be used for the final models. The 0.1 mm mesh has more than double the number of elements than the 0.15 mm mesh. For both SST $k-\omega$ and Re. $k-\epsilon$, the difference in pressure drop between the 0.1 mm and 0.15 mm base sizes is less than 3%. In order to keep future models from becoming prohibitively large, the 0.15 mm base size was chosen as the preferred base size.

2.4. Prism Layer

With base size chosen, the next step in selecting an optimal mesh was to determine the prism layer thickness. The prism layer should be sufficiently fine and thick to capture the wall effects. The number of prism layers was held at 10, as not to significantly change the number of elements in the mesh. Prism layer thicknesses of 0.05 mm, 0.1 mm, and 0.2 mm were tested. Figure 4 depicts the outlet cross section mesh for each base size. Table III. details the results for each turbulence model and base size, including pressure drop, percent difference from Chen and Todreas correlation, elements in mesh, approximate residuals, maximum y^+ value, and average y^+ value.

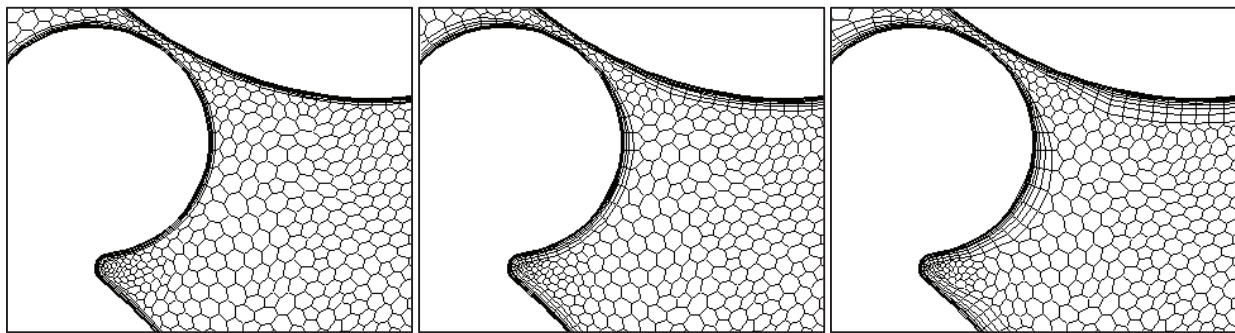


Figure 4. Mesh samples. Prism layer thickness left to right: 0.05 mm, 0.1 mm, 0.2 mm

Table III. Spatial Convergence Results

Turbulence Model	Prism Layer Thickness (mm)	Pressure Drop (Pa/cm)	% diff. from C&T	Elements (million)	Residuals	Max y^+	Avg. y^+
SST $k-\omega$	0.05	76.0	15.8	30.0	<1E-4	1.07	0.30
	0.1	85.2	5.6	29.3	<1E-4	1.10	0.32
	0.2	85.4	5.4	28.2	<1E-5	1.14	0.32
Re. $k-\epsilon$	0.05	94.8	5.0	30.0	<1E-3	1.07	0.34
	0.1	99.4	10.1	29.3	<1E-3	1.09	0.35
	0.2	99.9	10.6	28.2	<1E-3	1.14	0.35
C&T	-	90.3	-	-	-	-	-
Nov.	-	103.5	14.6	-	-	-	-
Rehme	-	93.3	3.4	-	-	-	-

A prism layer thickness of 0.05 mm significantly effects the results. This is most likely because it does not capture the entire boundary layer. The 0.1 mm and 0.2 mm prism layer thicknesses differ negligibly. The maximum y^+ values of each is greater than 1 which is undesirable. However, upon inspection of the models, this maximum value occurs at the entrance and most likely arises due to the low quality inlet conditions. The average y^+ value indicates that the boundary layer is resolved sufficiently. The similarity in y^+ values between the 0.1 mm and 0.2 mm prism layer thickness models indicates that the increased resolution near the boundary with 0.1 mm prism thickness is unnecessary. Additionally, the 0.2 mm prism layer thickness mesh requires slightly fewer elements. Thus, a prism layer thickness of 0.2 mm was chosen for the final mesh.

2.5. Inlet Condition

In order to obtain accurate results from the model, a fully developed inlet conditions must be used. Turbulence becomes fully developed at a length of about 10-100 times the hydraulic diameter [16]. One period of rotation should be enough to achieve fully developed turbulent flow. For optimal results, a model with an identical mesh with a length of one period of rotation should be used to create a fully developed inlet condition. However, as the inlet model is 6 times larger than the model used to find pressure drop, this inlet model would take ~6 times longer to model. For the larger domains intended to be modeled, this would take a prohibitively long computation time. Therefore it is preferred that a simpler model is used to find an approximate inlet condition. The simpler inlet condition, however, must first be shown to have little effect on the estimated pressure drop.

In this section two inlet conditions are compared for the SST $k-\omega$ and the Re. $k-\epsilon$ turbulence models. Two meshes were created for each model. The first inlet mesh uses the meshing parameters established in the previous sections. The second is a coarser mesh using a base size of 0.3 mm, a prism layer thickness of 0.1 mm and 5 prism layers. Identical prism layer thicknesses would be preferred, but the coarser mesh could not be created with a prism layer thickness of 0.2 mm as the meshing process failed. The two inlet meshes were then run with each turbulent model in order to create an inlet condition for the pressure drop calculation. The inlet conditions consisted of the x, y, and z velocity components as well as the turbulent viscosity ratio. The pressure drops were then calculated with each turbulence model using the two inlet conditions of the same turbulence model. A plot of each inlet condition's velocity magnitude distribution and turbulent viscosity ratio distribution are shown in figure 5. Table IV. details the results for each inlet condition and turbulence model, including pressure drop, percent difference from Chen and Todreas correlation, elements in inlet mesh, approximate residuals, average inlet velocity, and average turbulent viscosity ratio.

Table IV. Coarse and Fine Inlet Results

Turbulence Model	Inlet Mesh	Pressure Drop (Pa/cm)	% diff. from C&T	Inlet Elements (million)	Residuals	Avg. Vel. (m/s)	Avg. Turbulent Viscosity Ratio
SST $k-\omega$	Coarse	90.6	0.4	33.6	<1E-5	2.00	11.45
	Fine	96.2	6.6	168.3	<1E-5	2.01	15.05
Re. $k-\epsilon$	Coarse	106.0	17.4	33.6	<1E-3	2.00	6.70
	Fine	102.8	13.9	168.3	<1E-3	2.01	7.58
C&T	-	90.3	-	-	-	-	-
Nov.	-	103.5	14.6	-	-	-	-
Rehme	-	93.3	3.4	-	-	-	-

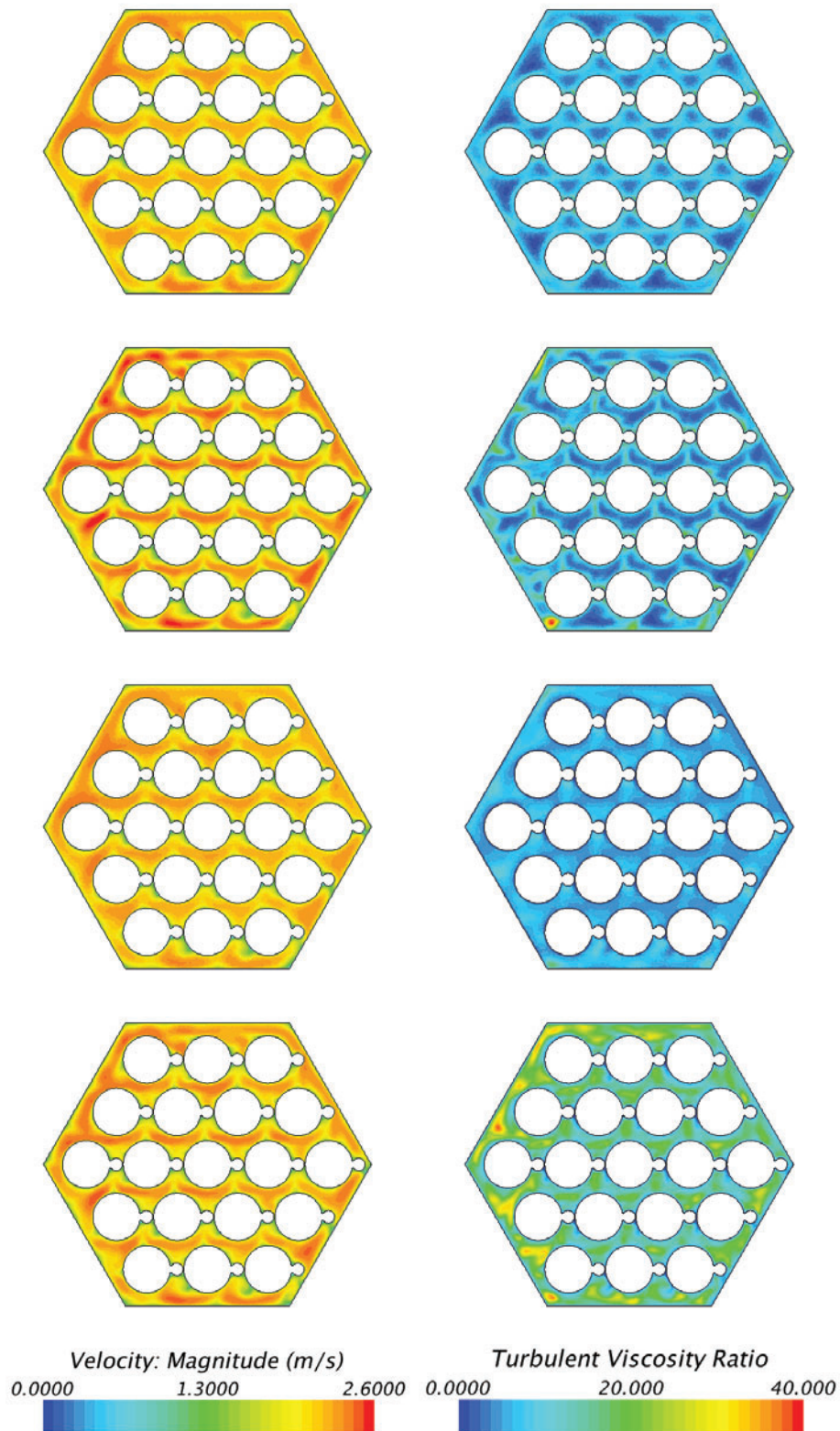


Figure 5. Velocity magnitude (left) and turbulent viscosity ratio (right) inlet distributions. From top to bottom: coarse re. $k-\epsilon$, fine re. $k-\epsilon$, coarse SST $k-\omega$, fine SST $k-\omega$

The finer inlet conditions display greater velocity gradients than the coarser meshes. This is because the finer mesh is able to better resolve the velocity gradients. The SST $k-\omega$ coarse inlet velocity and turbulent viscosity ratio distributions appear to better capture the higher and lower magnitudes that are apparent in the finer meshes. The re. $k-\epsilon$ inlet conditions show less agreement between the fine and coarse mesh than the SST $k-\omega$ inlet conditions. Qualitatively the SST $k-\omega$ coarse inlet condition appears to be a better approximation than the re. $k-\epsilon$ coarse inlet condition.

The difference in estimated pressure drop between the coarse and fine meshes is ~5% for both SST $k-\omega$ and re. $k-\epsilon$ turbulence models. This pressure drop comes with a 5 time reduction in number of elements in the inlet mesh, and therefore ~5 time reduction in computation cost. This tradeoff was considered to be acceptable for this study, which would otherwise be infeasible without access to higher power computational facilities.

With the meshing and inlet condition methods selected, the turbulence model for the subsequent bundle size sensitivity study was chosen. The SST $k-\omega$ turbulence model was selected over re. $k-\epsilon$ model for its better agreement with the C&T correlation, its smaller residuals, and its better approximate inlet conditions.

3. FUEL ROD BUNDLE SIZE COMPARISON

Fuel rod bundles of 19, 37, and 61 wire wrapped fuel rods were studied. Literature states that the 19 pin bundle is the smallest domain that effectively captures all relevant cross-flows between subchannels as the center channel is sufficiently insulated from the wall effects of the shroud [9]. The velocity distributions of the three bundles modeled are compared. The calculated pressure drops of the bundles are compared against empirical pressure drop models.

The meshing and inlet conditions for the 37 and 61 pin bundles were created using the methods outlined in the previous sections. All geometric parameters remain the same with the exception of wall length, which is increased to accommodate the additional fuel pins. The 37 pin bundle wall length is 31.115 mm, and the 61 pin bundle wall length is 39.515 mm.

3.1. Simulation Results and Analysis

The pressure drop of each model was the primary parameter for comparison and validation. The velocity distribution and turbulent viscosity ratio distribution were also found for qualitative comparison. Table V details the results for each bundle, including pressure drop, percent difference from Chen and Todreas correlation, elements in mesh, and approximate residuals. Figure 6 gives a plot of predicted pressure drop for this study's model, along with the empirical pressure drop correlations of Rheme, Novendstern, and Chen and Todreas.

Table V. Bundle Size Pressure Drop Results

Bundle Size	Pressure Drop (Pa/cm)	% diff. from C&T	Elements (million)	Residuals
19	90.6	0.4	28.2	<1E-5
37	92.6	3.5	51.9	<1E-5
61	93.4	4.8	82.7	<1E-5

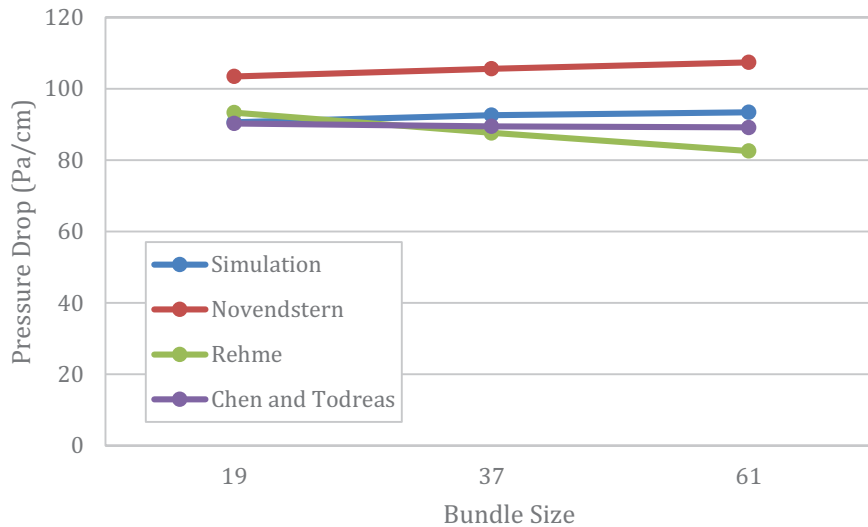
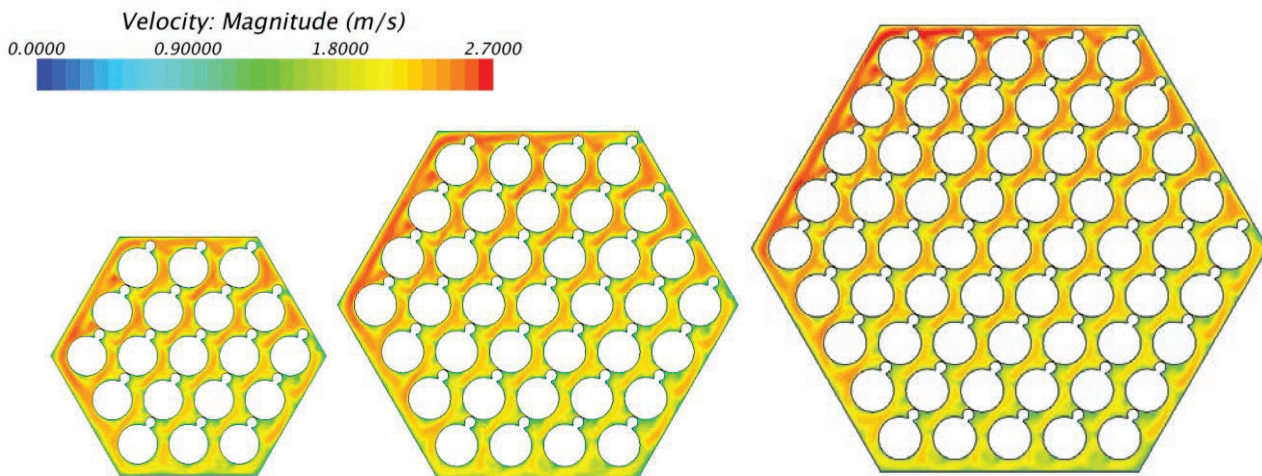


Figure 6. Modeled pressure drop and empirical correlations' pressure drop estimates

The three empirical correlations used in this investigation exhibit different behavior with increasing bundle size. Novendstern predicts an increase in pressure drop, Rehme predicts a substantial decrease in pressure drop, and Chen and Todreas predicts a slight decrease in pressure drop. As mentioned before, literature holds that the Chen and Todreas pressure drop correlation is the most accurate, so validation was done against the Chen and Todreas correlation. A slight drop in pressure with increased bundle size is expected. The smaller the bundle, the greater the percentage of subchannels affected by the shroud. The subchannels affected by the shroud have a smaller hydraulic diameter and so a greater pressure drop. As the bundle size increases, this shroud effect should decrease and pressure drop should level out with increasing bundle size. The simulated model, however did not exhibit this behavior. Pressure drop across more bundles of increased size should be found before the pressure drop data can be extrapolated to a fuel rod sub-assembly (typically 217 fuel rods). While the trend in pressure drop with bundle size did not match that of the Chen and Todreas correlation, the pressure drops were within 5% agreement. Figure 7 gives the velocity and turbulent viscosity distributions at the outlet for each bundle size.



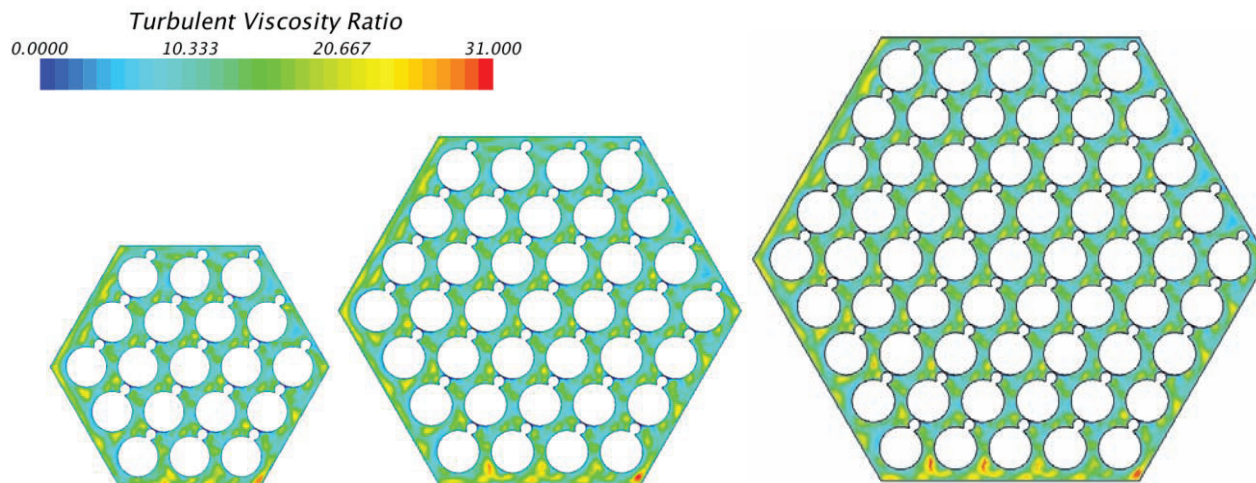


Figure 7. Exit velocity (top) and turbulent viscosity ratios (bottom) for each bundle size

Qualitatively each bundle size shows the same behavior of increased fluid flow on the top left side, and decreased in the bottom right. The same pattern of flow appears in all interior subchannels. The larger rod bundles show a greater disparity in flow rate. This increased flow rate through exterior subchannels for larger rod bundles explains the increase in pressure drop with increased bundle size. In the each pin bundle the top left interior subchannels appear to have a substantially greater average velocity than the bottom right subchannels. This indicates that a certain number of buffer layers may be necessary to isolate interior subchannels from the wall effect. The turbulent viscosity ratios show the same patterns in each bundle. There appears to be little difference in distribution for the interior subchannels. A qualitative examination suggests that the interior subchannel velocity magnitudes may be affected by the wall. The severity of the effect and the bundle size necessary to diminish the effect for interior channels can be found with a more quantitative analysis.

The objective of this study is to find the minimum bundle size such that the behavior at the most center subchannels have no dependence on bundle size. The average subchannel velocity at the outlet was taken to be representative of subchannel behavior. The hexagonal subchannel bundle is broken into zones based

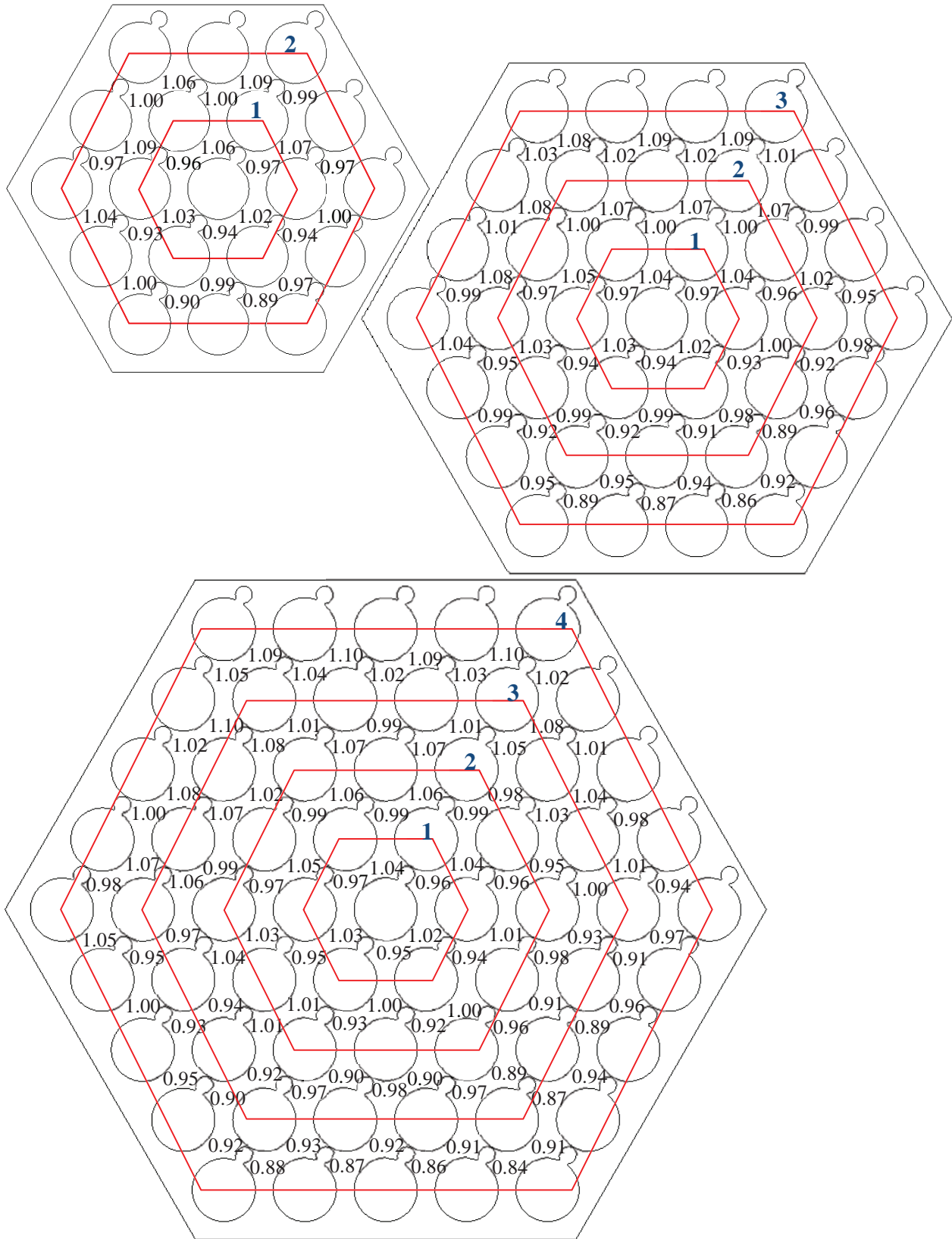


Figure 8. Average interior subchannel velocity ratio for 19 (top), 37 (middle), and 61 (bottom) pin bundles

on subchannel distance from the center. The zones are shown in figure 8. Figure 8 gives for each subchannel the ratio of the average subchannel velocity magnitude to the total average velocity. A difference in subchannel velocity ratios between bundles for any zone indicates that the subchannels in that zone are not independent of bundle size. The average percent difference of zones in the 19 pin and 37 pin bundle from the 61 pin bundle are given in Table VI.

Table VI. Bundle Size Pressure Drop Results

Bundle Size	Percent Difference from 61 pin bundle		
	Zone 1	Zone 2	Zone 3
19	0.68 %	1.66 %	-
37	0.28 %	0.96 %	1.75 %

For this analysis, a percent difference of less than 1% is considered independent of wall effects. Thus in a bundle size of 19, the innermost subchannels are independent of wall effects. In a bundle size of 37, the two innermost zones are independent of wall effects. In both cases, a single zone is necessary to act as a buffer to the wall effects. Zone 1 in the 37 pin bundle is the only example in this study with two buffers. Its results indicate that additional buffer zones may increase the independence from bundle size. Larger pin bundles would need to be modeled to determine the effect of additional buffer zones. The minimum bundle size for independence of grid size for the innermost subchannels is 19 pins, which is in agreement with the findings of Gajapathy [9].

4. CONCLUSIONS

The purpose of this study was to establish a procedure for meshing and simulating flow through a wire wrapped fuel rod bundle. The procedure was validated against empirical correlations for pressure drop. The chosen turbulence model was the SST (Menter) $k-\omega$ turbulence with low y^+ treatment. Care was taken to resolve the boundary layer with minimal use of wall functions. With the procedure established, pin bundles with 19, 37, and 61 pins were modeled steady state to find the velocity distribution and pressure drop for each bundle size. The velocity distribution was first qualitatively analyzed which revealed that each bundle exhibited similar behavior, however the internal subchannels appeared to be affected by the wall effects. The magnitude of the wall effects were then studied by comparing the subchannel velocities for the different bundles. The centermost subchannels of the 19 pin bundle differ in velocity on average by less than 1% from the centermost subchannels of the 61 pin bundle. The subchannels in the two centermost zones of the 37 pin bundle differ in velocity on average by less than 1% from the corresponding subchannels of the 61 pin bundle. The average subchannel velocity is approximately independent from bundle size for said subchannels. For the 19 pin bundle 6 of the 42 subchannels are independent of bundle size. For the 37 pin bundle 24 of the 78 subchannels are independent of bundle size. A single layer of subchannels between the wall and interior subchannels was sufficient to isolate interior subchannels from wall effects. An additional buffer layer was shown to increase accuracy of interior subchannels, however larger bundles must be simulated to study the effects of additional buffer layers.

ACKNOWLEDGMENTS

The authors acknowledge the Texas A&M Supercomputing Facility (sc.tamu.edu) for providing computing resources useful in conducting the research reported in this paper.

REFERENCES

1. D.S. Rowe, "COBRA IIIC: A Digital Computer Program for Steady-State and Transient Thermal Analysis of Rod Bundle Nuclear Fuel Elements" BNWL-1695, Pacific Northwest Laboratory, 1973.
2. T.H. Fanning et al., "Multi-Resolution Modeling of Subassembly Pin Bundles for Advanced Fast Reactor Safety Simulations," *Proceedings of 2009 International Conference on Mathematics, Computational Methods & Reactor Physics (M&C 2009)*, Saratoga Springs, New York, May 3-7, 2009 (2009).
3. K.D. Hamman and R.A. Berry, "A CFD Simulation Process for Fast Reactor Fuel Assemblies," *Nuclear Engineering and Design*, **240**(9), pp. 2304-2312 (2010).
4. W. Raza and K.Y. Kim, "Effects of Wire-Spacer Shape on LMR on Thermal-Hydraulic Performance," *Nuclear Engineering and Design*, **238**(10), pp. 2678-2683 (2008).
5. K. Natesan et al., "Turbulent Flow Simulation in a Wire-Wrap Rod Bundle of an LMFBR," *Nuclear Engineering and Design*, **240**(5), pp. 1063-1072 (2010).
6. P. Fischer et al., "Large Eddy Simulation of Wire-Wrapped Fuel Pins I: Hydrodynamics in a Periodic Array," *Proceedings of 2007 Joint International Topical Meeting on Mathematics & Computation and Supercomputing in Nuclear Applications (M&C + SNA 2007)*, Monterey, California, April 15-19, 2007 (2007).
7. J.G. Smith et al., "Effects of Mesh Density and Flow Conditioning in Simulating 7-Pin Wire Wrapped Fuel Pins," *Proceedings of 16th International Conference on Nuclear Engineering (ICONE16)*, Orlando, Florida, May 11-15, 2008 pp. 755-763 (2008).
8. E. Merzari et al., "Numerical Simulation of the Flow in Wire-Wrapped Pin Bundles: Effect of Pin-Wire Contact Modeling," *Nuclear Engineering and Design*, **253**, pp. 374-386 (2012).
9. R. Gajapathy et al., "A Comparative CFD Investigation of Helical Wire-Wrapped 7, 19 and 37 Fuel Pin Bundles and its Extensibility to 217 Pin Bundle," *Nuclear Engineering and Design*, **239**(11), pp. 2279-2292 (2009).
10. K. Rehme, "Pressure Drop Correlations for Fuel Element Spacers," *Nuclear Technology*, **17**, pp. 15-23 (1973).
11. E.H. Novendstern, "Turbulent Flow Pressure Drop Model for Fuel Rod Assemblies Utilizing a Helical Wire-Wrap Spacer System," *Nuclear Engineering and Design*, **22**(1), pp. 28-42 (1972).
12. S.K. Cheng and N.E. Todreas, "Hydrodynamic Models and Correlations for Bare and Wire-Wrapped Hexagonal Rod Bundles," *Nuclear Engineering and Design*, **92**(2), pp. 227-251 (1986).
13. S.K. Chen, N.E. Todreas, and N.T. Nguyen, "Evaluation of Existing Correlations for the Prediction of Pressure Drop in Wire-Wrapped Hexagonal Array Pin Bundles," *Nuclear Engineering and Design*, **267**, pp. 109-131 (2014).
14. M.H. Chun et al., "An Experimental Study of Pressure Drop Correlations for Wire-Wrapped Fuel Assemblies," *KSME International Journal*, **15**(3), pp. 403-409 (2001).
15. J.K. Fink and L. Leibowitz, "Thermodynamic and Transport Properties of Sodium Liquid and Vapor" ANL/RE-95/2, Argonne National Laboratory, 1995.
16. N.E. Todreas and M.S. Kazimi, *Nuclear Systems Volume 1: Thermal Hydraulics Fundamentals*, Ch 9, CRC Press, New York (2012).